Low-temperature Hall effect in electron-doped superconducting La$_{2-x}$Ce$_x$CuO$_4$ thin films

K. Jin, B. Y. Zhu, B. X. Wu, L. J. Gao, and B. R. Zhao[*]

National Laboratory for Superconductivity, Beijing National Laboratory for Condensed Matter Physics,
and Institute of Physics, Chinese Academy of Sciences, Beijing 100080, China

We investigate the low-temperature Hall effect in electron-doped La$_{2-x}$Ce$_x$CuO$_4$ thin films from heavily underdoped $x=0.06$ to heavily overdoped $x=0.17$. With increasing x, the charge carriers that dominate the Hall effect gradually change from electronlike to holelike. From the Hall coefficient and differential Hall coefficient, we infer that a large holelike Fermi surface forms above $x=0.15$, that is, the electronlike pocket may exist until $x=0.15$. Meanwhile, the sign of the Hall resistivity changes from negative ($x=0.105$) to positive ($x=0.12$) at 2 K, indicating that single electron pocket exists below $x=0.105$ at low temperature.

Transport measurements are frequently carried out to reveal the electronic structure of high-T_c cuprate superconductors (HTSs), such as the phase transition,[1–3] the quantum critical point (QCP),[4–6] the stripe order,[7] and the origin of the pseudogap.[8] Quantum oscillations of resistivity and Hall resistivity have been observed in underdoped YBa$_2$Cu$_3$O$_{6.5}$ (Ref. 9) and the reconstruction of the Fermi surface (FS) is demonstrated.[10] The resistivity in high magnetic fields is used to characterize energy scales of the two-dimensional (2D) local paring in YBa$_2$Cu$_3$O$_{6.6}$ crystals.[11] Studies on electron-doped Pr$_{2-x}$Ce$_x$CuO$_4$ (PCCO) thin films reveal that the upturn of resistivity is due to the spin scattering[12] and spin-density wave (SDW) induced FS reconstruction model is responsible for the anomalous Hall effect and magnetoresistivity in high magnetic fields.[13]

Recently, the high-temperature Hall effect of HTS has been performed on the parent insulator of the electron-doped system.[14] The Hall coefficient (R_H) of Pr$_{1.3}$La$_{0.7}$CuO$_4$ shows sign reversal near 700 K, above which R_H is positive. Previously, Onose *et al.*[15] pointed out that in underdoped Nd$_{2-x}$Ce$_x$CuO$_4$ (NCCO) the FS is holelike at high temperature and gradually evolves into holelike and electronlike pockets as the temperature decreases, then into a single electronlike pocket. This process is similar to the evolution of FS with decreasing Ce doping revealed by the angle-resolved photoemission spectroscopy (ARPES) experiments.[16] In order to reveal the ground state of electron-doped HTS, low-temperature Hall effect has been addressed for PCCO system and a kink of $R_H(x)$ at 0.35 K has been observed between $x=0.16$ and 0.17, hereby a QCP is suggested to exist in this range.[6]

In electron-doped HTS family, the optimal doping of La$_{2-x}$Ce$_x$CuO$_4$ (LCCO) is ~0.10–0.11,[3,17,18] quite different from that of NCCO and PCCO systems (both around 0.15). Therefore, it is interesting to test whether the quantum phase transition due to FS rearrangement lies on the optimal doping or reflects the common mechanism of electron-doped HTS, that is, whether the larger holelike FS forms. In present work, we systematically investigate the low-temperature (down to 2 K) Hall effect in LCCO thin films. We find that with increasing x from underdoped $x=0.06$ to overdoped $x=0.17$, the charge carriers that dominate the Hall effect gradually change from electronlike to holelike, consistent

with the ARPES results.[16,19] Further, we infer that a large holelike FS forms above $x=0.15$, that is, the electronlike pocket may exist until $x=0.15$. The sign of $\rho_{xy}(H)$ at 2 K changes from negative ($x=0.105$) to positive ($x=0.12$), indicating that single electronlike pocket exists below $x=0.105$ at low temperature.

All the LCCO films for the present study were prepared by dc magnetron sputtering method.[20,21] To obtain LCCO thin films with high quality, we carefully adjusted the deposition temperature, the ratio of Ar to O$_2$, and the annealing process for each doping level. Owing to the undetermined oxygen content in films, we chose the highest T_c and sharp transition of the annealed films for each Ce content. The 100 nm thin films were patterned into bridges with six terminals by photolithography and Ar-ion milling for both resistivity (ρ_{xx}) and Hall resistivity (ρ_{xy}) measurements. Some parameters of the films are listed in Table I. T_{c0}, T_c^{onset}, and T_{min} represent the temperatures of zero resistance transition, onset of superconducting transition, and minimum ρ_{xx} (Ref. 22) in zero magnetic field, respectively. The main features are that (i) the films with $x \geq 0.09$ are superconducting, (ii) the highest T_c^{onset} appears at $x=0.09$, while the sharpest transition and highest T_{c0} are at $x=0.105$, and (iii) the normal-state ρ_{xx} decreases as x increases.

TABLE I. T_{c0}, T_c^{onset}, T_{min}, and ρ_{xx} for different doping levels. T_{c0}, T_c^{onset}, and T_{min} represent the temperatures of zero resistance transition, onset of superconducting transition, and minimum ρ_{xx} in zero magnetic field, respectively.

x	T_{c0} (K)	T_c^{onset} (K)	T_{min} (K)	ρ_{xx} ($\mu\Omega$ cm) [a]
0.06			90	2700
0.08			88	360
0.09	22.5	29		273
0.105	26.5	28		190
0.12	19	22		138
0.13	16	19		124
0.15	12	16		75
0.17	3	8		16

[a]ρ_{xx} at 100 K.
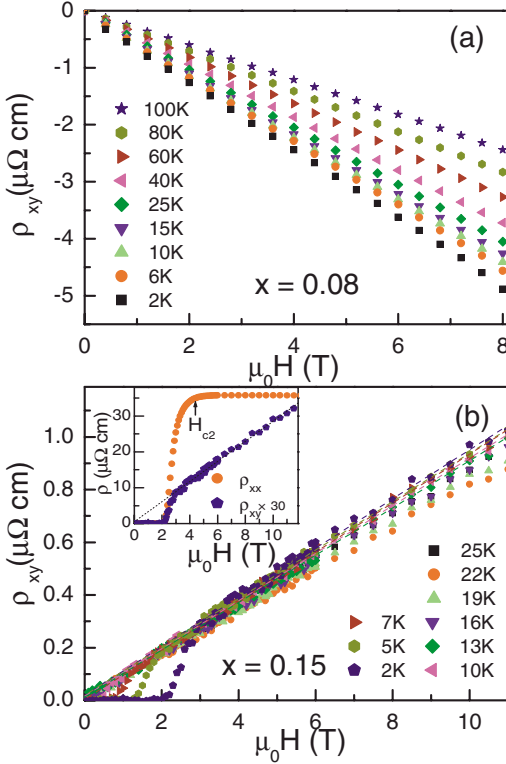
FIG. 1. (Color online) The Hall resistivity $\rho_{xy}(H)$ of (a) underdoped $x=0.08$ and (b) overdoped $x=0.15$. ρ_{xy} is proportional to H for both samples in the normal state. Inset: $\rho_{xx}(H)$ and 30 times enlarged $\rho_{xy}(H)$ at 2 K for $x=0.15$. The black arrow points to H_{c2}.

We first describe the $\rho_{xy}(H,T)$ curves of different doping levels. For the underdoped region, the ρ_{xy} of the nonsuperconducting LCCO thin films with $x=0.06$ and 0.08 is negative and proportional to the magnetic field. As seen in Fig. 1(a), the films with $x=0.08$ show $\rho_{xy} \propto H$ at different temperatures from $>T_{min} \sim 88$ K down to 2 K. In the overdoped region, the ρ_{xy} of $x=0.15$ and 0.17 films is linear with the magnetic field in normal state, and the linear region of $\rho_{xy}(H)$ could be extrapolated well to the origin of the coordinates. The $\rho_{xy}(H)$ curves of $x=0.15$ are presented in Fig. 1(b). It is clear that the fitted dashed lines pass well through the origin. Therefore, the $\rho_{xy} \propto H$ relation is also held well in the normal state of the overdoped $x=0.15$ and 0.17, while ρ_{xy} is positive. Since $\rho_{xy} \propto H$ is similar to the behavior within the framework of conventional one-band Drude model, we infer that the electronlike (holelike) charge carriers completely dominate the Hall effect in the heavily underdoped (overdoped) region.

From $x=0.09$ to 0.13, the $\rho_{xy}(H,T)$ shows dramatic change with varying H and T, especially near the optimal doping. The $\rho_{xy}(H)$ curves of all these superconducting films show linear part at low temperatures in certain high-field regime, whereas the extrapolated linear part of $\rho_{xy}(H)$ does not pass the origin, i.e., ρ_{xy} is linear with H ($\sim H$) but not proportional to H ($\propto H$). We take $x=0.105$ for example. The T_{c0} and T_c^{onset} of $x=0.105$ are ~ 26.5 and 28 K, respectively (as seen in Fig. 2). The $\rho_{xy}(H)$ curves of $x=0.105$ are shown in Fig. 3(a). At 2 K, the $\rho_{xy}(H)$ is zero in low-field regime and becomes negative as H increases. The linear part of $\rho_{xy}(H)$ could be observed from 9 to 12 T. To see it clearly, we
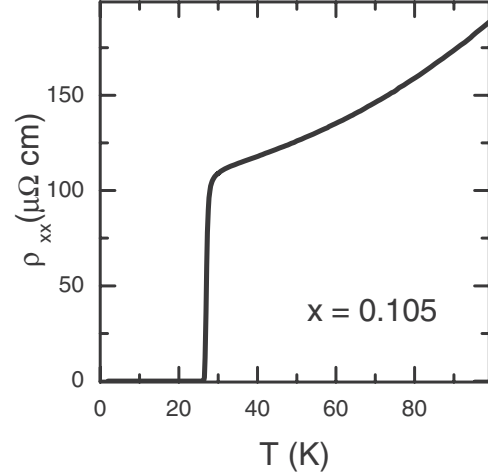
FIG. 2. The $\rho_{xx}(T)$ of $x=0.105$ in zero magnetic field.

plot the differential $\rho_{xy}(H)$, i.e., $d\rho_{xy}/dH(=R_H')$ in Fig. 3(b). The constant value of R_H' between 9 and 12 T reflects the linear part rightly. Note that all the fitted dashed lines do not pass the origin. As T increases, the onset of the linear part shifts toward lower fields and deviation from linearity appears in higher fields [cf. dashed lines in Fig. 3(a)]. The relationship between ρ_{xy} and H gradually changes from $\rho_{xy} \sim H$ to $\rho_{xy} \sim H^2$. In Fig. 3(c), ρ_{xy} is plotted as the function of H^2. It is obvious that $\rho_{xy} \sim H^2$ is held very well nearly in the whole field regime.

In our previous work, we have reported the transport properties of LCCO films with $x=0.11$.[20] Compared to $x=0.11$, the $\rho_{xy}(H,T)$ of $x=0.105$ shows some similarities, including twice sign reversals and $\rho_{xy} \sim H^2$ behavior at mediate temperatures. However, the positive $\rho_{xy}(H,T)$ region is narrower in $x=0.105$ than in $x=0.11$. In Fig. 4, we plot the $\rho_{xy}(T)$ curves of $x=0.105$ and 0.11 at $H=5$ and 10 T. Obviously, the $\rho_{xy}(T)$ curves of $x=0.11$ have broader positive region and larger field is needed to suppress the positive region. This means that the holelike charge carriers play a more important role in the Hall resistivity of $x=0.11$ than
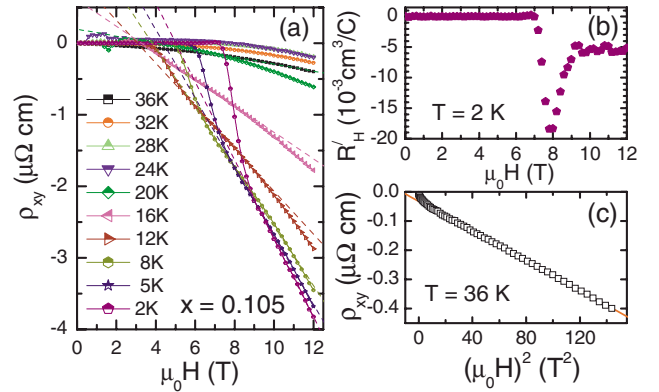
FIG. 3. (Color online) (a) The Hall resistivity $\rho_{xy}(H)$ of $x=0.105$. The dashed lines are fit for the linear part of $\rho_{xy}(H)$. (b) Differential Hall coefficient R_H' ($=d\rho_{xy}/dH$) at 2 K. The constant R_H' in the region of 9–12 T means $\rho_{xy}\sim H$. (c) ρ_{xy} vs H^2 at 36 K, where $\rho_{xy} \sim H^2$ is held well in rather wide field range.
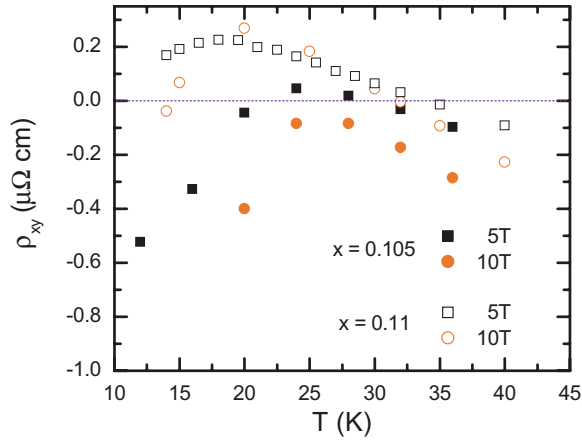
FIG. 4. (Color online) ρ_{xy} versus T curves of $x=0.105$ and 0.11 at $H=5$ and 10 T.

that of $x=0.105$. This is because the holelike charge carriers gradually dominate the transport properties with increasing x. Note that the positive $\rho_{xy}(H,T)$ region is broader in $x=0.11$ than in $x=0.105$ but narrower in $x=0.12$. The $\rho_{xy}(H,T)$ of $x=0.12$ is positive in the whole investigated region of (2–22 K, 0–12 T) as shown in Fig. 5.

To get the full image of $\rho_{xy}(H,T,x)$, we plot the contour maps of $\rho_{xy}(H,T)$ for $x=0.09, 0.105, 0.12,$ and 0.13 in Fig. 5. The crosses in Fig. 5 represent the upper critical field H_{c2} obtained from the differential $\rho_{xx}(H)$ curves (discussed below). For the slightly underdoped $x=0.09$ [Fig. 5(a)], the $\rho_{xy}(H,T)$ is negative in the normal state, and a small positive region can be observed in the mixed state. In Fig. 5(b), the $\rho_{xy}(H,T)$ of $x=0.105$ shows broader positive region than that of $x=0.09$, which expands to cross the H_{c2}, indicating the contribution of holelike charge carriers is enhanced.[20] The $\rho_{xy}(H,T)$ of $x=0.12$ and 0.13 is positive in the whole investigated region, whereas for $x=0.12$ the $\rho_{xy}(H)$ first increases and then decreases with increasing H at $T<6$ K (as seen
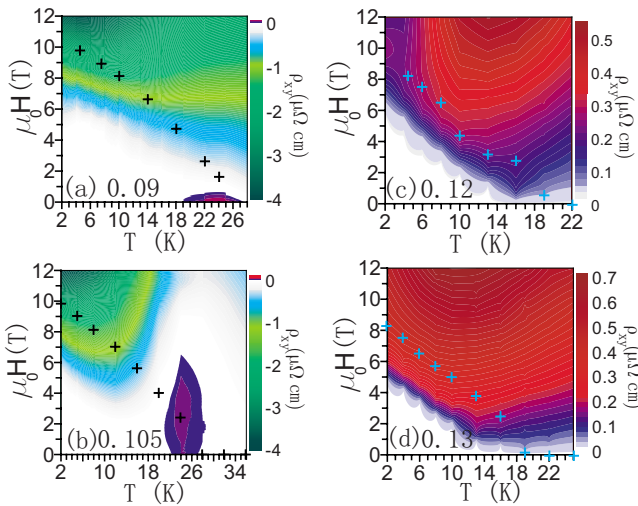
FIG. 5. (Color online) Contour maps of $\rho_{xy}(H,T)$ for (a) $x=0.09$, (b) 0.105, (c) 0.12, and (d) 0.13. The sign and magnitude of $\rho_{xy}(H,T)$ could be distinguished by color bars. The crosses in each panel demonstrate the H_{c2}.
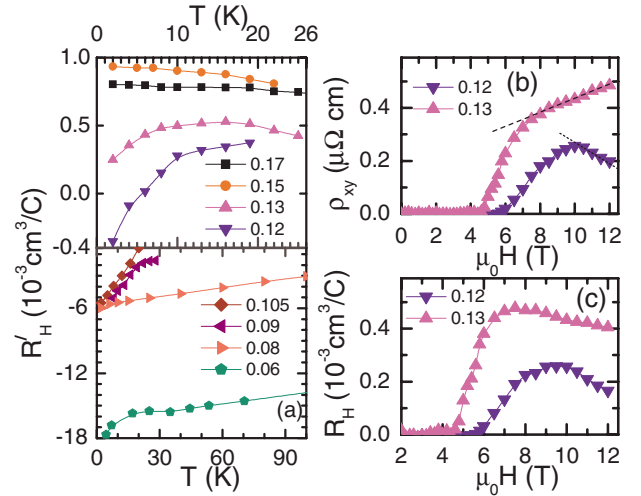
FIG. 6. (Color online) (a) Temperature dependent of $R_H'(=d\rho_{xy}/dH)$ obtained from the linear part of $\rho_{xy}(H)$. Note that the upper and lower panels are in different temperature ranges. (b) $\rho_{xy}(H)$ and (c) R_H of LCCO films with $x=0.12$ and 0.13 at 2 K.

clearly in Fig. 6), which implies the contribution of electronlike charge carriers is increased with increasing H. It is undoubted that the charge carriers that dominate the Hall resistivity change from electronlike to holelike with increasing x, and the behavior of previously investigated $x=0.11$ just mediates between 0.105 and 0.12.

Then we turn to describing the Hall coefficient R_H in these LCCO films. For $x=0.06, 0.08, 0.15,$ and 0.17, the R_H is constant for different magnetic fields because of $\rho_{xy}\propto H$, while for other films with $0.09\leq x\leq0.13$, R_H varies with different fields. So we also define the differential Hall coefficient $R_H'=d\rho_{xy}/dH$, which is obtained from the linear part of $\rho_{xy}(H)$ in these doping levels. First, we compare the R_H and R_H': for $x=0.06, 0.08, 0.15,$ and 0.17, $R_H=R_H'$ due to $\rho_{xy}\propto H$; for $0.09\leq x\leq0.13$, we assume $\rho_{xy}=a+bH$ for the linear part of the $\rho_{xy}(H)$ with a and b as constants for each $\rho_{xy}(H)$ curve. It is interesting that the values of a for $0.09\leq x\leq0.13$ are always positive, so $R_H=a/H+b$ is always larger than $R_H'(=b)$ and decreases with increasing H. At low temperatures ρ_{xy} shows linearity with H in high-field regime; we may get the information about which kind of charge carriers begins to dominate the transport and how the dominant charge carriers change as x increases.

Figure 6(a) shows $R_H'(T,x)$. It can be seen that for the films with $x=0.06$, the $R_H'(T)$ is negative and decreases with decreasing T, and a quick drop can be observed at low temperature. For $x=0.08, 0.09,$ and 0.105, the $R_H'(T)$ is negative and also decreases as T decreases; for $x=0.12$ and 0.13, their values of $R_H'(T)$ first increase and then decrease with decreasing T. The difference is that $R_H'(T)$ of $x=0.12$ changes from positive to negative at low temperature. We mention that the $\rho_{xy}(H)$ of $x=0.12$ first increases and then decreases with increasing field at low temperature as seen in Fig. 6(b). The negative $R_H'(T)$ of $x=0.12$ is obtained from the linear part of $\rho_{xy}(H)$ in the high-field regime [the dashed line in Fig. 6(b)]. Hence, this means that the contribution of the electronlike charge carriers to the Hall effect is enhanced though the Hall coefficient is still positive as shown in Fig.

6(c). For $x=0.15$ and 0.17, $R_H'(T)$ is positive and nearly keeps constant in $x=0.17$ with decreasing T, in contrast with the slowly increase in $x=0.15$. This implies that holelike FS forms for $x \geq 0.15$, compatible with the single large hole pocket seen by ARPES in overdoped NCCO.[23]

Theory for electron-doped HTS predicts that the FS is rearranged below a critical value x_c due to a commensurate SDW order, and below a lower critical value x_1 the hole pockets are eliminated.[24] According to the theory, the x_c in LCCO, where the large holelike FS is rearranged, is likely between $x=0.15$ and 0.17. The Hall coefficient changes from negative to positive at $x=0.105$ at 2 K, so we infer x_1 is near 0.105. Note that the $R_H (=R_H')$ of $x=0.15$ is larger than that of $x=0.17$; this is inconsistent with the theory predicted $R_H \sim 1/(1-x)$. However, we can understand the present results on the basis of the concentration of charge carriers. As seen in Table I, the resistivity is lower and lower with increasing doping, so it is reasonable that the concentration of holelike charge carriers increases when large holelike FS forms. Therefore, the R_H of $x=0.17$ is smaller due to larger concentration of holelike charge carriers. Besides, though the x_c in LCCO is similar to that in PCCO,[6] a plateau of $R_H'(x)$ is observed from $x=0.08$ to 0.105 and the maximum positive value appears at $x \sim 0.15$ instead of a kink observed in PCCO. One possible reason may be ascribed to different optimal doping ranges in these two systems. In addition, further work at much more lower temperature is required.

Finally, we simply demonstrate the method how we obtained the B_{c2}. As shown in Fig. 7, we find that the differential $\rho_{xx}(H)$ ($d\rho_{xx}/dH$) curves show maximum values at certain magnetic fields (B_p) at temperatures both below and above T_c^{onset}. At temperatures below T_c^{onset} the B_p can reflect vortex dynamics,[25] corresponding to the transition of vortex motion from plastic state to elastic bundle state.[26] The B_p at temperatures above T_c^{onset} should mainly be caused by other reasons rather than the superconductivity because the B_p can exist at temperature far higher than the transition temperature as seen in Fig. 7(a). In the inset of Fig. 1(b), we can see that $\rho_{xx}(H)$ increases slowly near the labeled H_{c2} in $x=0.15$. It is difficult to define where is the accurate $B_{c2}(T_1)$ just from single $d\rho_{xx}/dH(H)$ curve at $T=T_1$ even on logarithmic scale as seen in Fig. 7(b). So we reasonably assume the fast increase in $\rho_{xx}(H)$ is caused by vortex dynamics and the slow increase in $\rho_{xx}(H)$ in normal state is resulted from other reasons. The B_{c2} (crosses) in Fig. 5 is thus determined by the crossing points (CPs) of $d\rho_{xx}/dH(H,T)$ with the maximum of $d\rho_{xx}/dH(T_c^{onset})$ [for $x=0.15$ $T_c^{onset} \sim 16$ K, the CP of
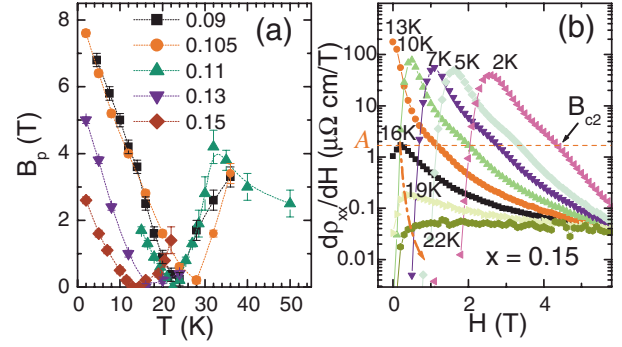
FIG. 7. (Color online) (a) Temperature dependence of B_p with different doping levels. B_p is defined as the field corresponding to the peak of $d\rho_{xx}/dH$ versus H. (b) Magnetic field derivative of the resistivity ($d\rho_{xx}/dH$) versus H. We take $x=0.15$, for example, to show how to obtain the upper critical field B_{c2}. Label A equals $d\rho_{xx}/dH(B_p, T_c^{onset}=16$ K$)$. The y-axis is plotted on logarithmic scale.

$d\rho_{xx}/dH(H,T)$ with the dashed line (A)]. In PCCO, large normal-state Nernst signal was found from slightly underdoped to overdoped region, compatible with two-band model.[27] In LCCO, there are also evidences that two kinds of charge carriers participate in the transport such as sign reversal of ρ_{xy} in normal state[20] and $\rho_{xy} \sim H^2$ at moderate temperatures. So one possible explanation for B_p at temperatures above T_c^{onset} is due to two-band effect in electron-doped HTS. Note that A could change at temperatures far away from T_c^{onset}. However, the relative values of B_{c2} for different LCCO thin films seem to be reasonable.

In conclusion, the Hall effect in electron-doped LCCO thin films is investigated down to 2 K. The $\rho_{xy}(H)$ curves of heavily underdoped $x \leq 0.08$ and overdoped $x \geq 0.15$ obey $\rho_{xy} \propto H$ at low temperature, indicating that electronlike (holelike) charge carriers completely dominate the Hall effect in heavily underdoped (overdoped) region, respectively. For $0.09 \leq x \leq 0.13$, the ρ_{xy} is linear with H at lower temperatures and in high-field regime. From the Hall coefficient and differentiated Hall coefficient, we infer that the electronlike pocket exists until $x=0.15$, above which a large holelike FS forms. At 2 K, the $\rho_{xy}(H)$ changes from negative to positive just in a small doping region ($\Delta x \sim 0.015$), indicating that single electron-pocket exists for $x \leq 0.105$.

---

*brzhao@aphy.iphy.ac.cn

[1] G. S. Boebinger, Y. Ando, A. Passner, T. Kimura, M. Okuya, J. Shimoyama, K. Kishio, K. Tamasaku, N. Ichikawa, and S. Uchida, Phys. Rev. Lett. **77**, 5417 (1996).

[2] S. Ono, Y. Ando, T. Murayama, F. F. Balakirev, J. B. Betts, and G. S. Boebinger, Phys. Rev. Lett. **85**, 638 (2000).

[3] A. Sawa, M. Kawasaki, H. Takagi, and Y. Tokura, Phys. Rev. B **66**, 014531 (2002).

[4] Y. Ando and K. Segawa, Phys. Rev. Lett. **88**, 167005 (2002).

[5] Y. Ando, S. Ono, X. F. Sun, J. Takeya, F. F. Balakirev, J. B. Betts, and G. S. Boebinger, Phys. Rev. Lett. **92**, 247004 (2004).

[6] Y. Dagan, M. M. Qazilbash, C. P. Hill, V. N. Kulkarni, and R. L. Greene, Phys. Rev. Lett. **92**, 167001 (2004).

[7] T. Noda, H. Eisaki, and S.-I. Uchida, Science **286**, 265 (1999).

[8] Y. Onose, Y. Taguchi, K. Ishizaka, and Y. Tokura, Phys. Rev. Lett. **87**, 217001 (2001).

[9] N. Doiron-Leyraud, C. Proust, D. LeBoeuf, J. Levallois, J.-B. Bonnemaison, R. X. Liang, D. A. Bonn, W. N. Hardy, and L. Taillefer, Nature (London) **447**, 565 (2007).

[10] D. LeBoeuf, N. Doiron-Leyraud, J. Levallois, R. Daou, J.-B. Bonnemaison, N. E. Hussey, L. Balicas, B. J. Ramshaw, R. X. Liang, D. A. Bonn, W. N. Hardy, S. Adachi, C. Proust, and L. Taillefer, Nature (London) **450**, 533 (2007).

[11] F. Rullier-Albenque, H. Alloul, C. Proust, P. Lejay, A. Forget, and D. Colson, Phys. Rev. Lett. **99**, 027003 (2007).

[12] Y. Dagan, M. C. Barr, W. M. Fisher, R. Beck, T. Dhakal, A. Biswas, and R. L. Greene, Phys. Rev. Lett. **94**, 057005 (2005).

[13] P. C. Li, F. F. Balakirev, and R. L. Greene, Phys. Rev. Lett. **99**, 047003 (2007).

[14] S. Ono, S. Komiya, and Y. Ando, Phys. Rev. B **75**, 024515 (2007).

[15] Y. Onose, Y. Taguchi, K. Ishizaka, and Y. Tokura, Phys. Rev. B **69**, 024504 (2004).

[16] N. P. Armitage, F. Ronning, D. H. Lu, C. Kim, A. Damascelli, K. M. Shen, D. L. Feng, H. Eisaki, Z. X. Shen, P. K. Mang, N. Kaneko, M. Greven, Y. Onose, Y. Taguchi, and Y. Tokura, Phys. Rev. Lett. **88**, 257001 (2002).

[17] H. Wu, L. Zhao, J. Yuan, L. X. Cao, J. P. Zhong, L. J. Gao, B. Xu, P. C. Dai, B. Y. Zhu, X. G. Qiu, and B. R. Zhao, Phys. Rev. B **73**, 104512 (2006).

[18] M. Naito, S. Karimoto, and A. Tsukada, Supercond. Sci. Technol. **15**, 1663 (2002).

[19] H. Yamamoto, M. Naito, A. Tsukada, and S. Suzuki, Physica C **412–414**, 134 (2004).

[20] K. Jin, B. Y. Zhu, J. Yuan, H. Wu, L. Zhao, B. X. Wu, Y. Han, B. Xu, L. X. Cao, X. G. Qiu, and B. R. Zhao, Phys. Rev. B **75**, 214501 (2007).

[21] L. Zhao, H. Wu, J. Miao, H. Yang, F. C. Zhang, X. G. Qiu, and B. R. Zhao, Supercond. Sci. Technol. **17**, 1361 (2004).

[22] K. Jin, B. Y. Zhu, B. X. Wu, J. Vanacken, V. V. Moshchalkov, B. Xu, L. X. Cao, X. G. Qiu, and B. R. Zhao, Phys. Rev. B **77**, 172503 (2008).

[23] H. Matsui, T. Takahashi, T. Sato, K. Terashima, H. Ding, T. Uefuji, and K. Yamada, Phys. Rev. B **75**, 224514 (2007).

[24] J. Lin and A. J. Millis, Phys. Rev. B **72**, 214506 (2005).

[25] N.-C. Yeh, Phys. Rev. B **43**, 523 (1991).

[26] A. E. Koshelev and V. M. Vinokur, Phys. Rev. Lett. **73**, 3580 (1994).

[27] P. C. Li and R. L. Greene, Phys. Rev. B **76**, 174512 (2007).